*International Journal of Scientific Research and Modern Technology (IJSRMT)* *ijsrmt.com*
*Volume 5, Issue 6, 2026*
*DOI: https://doi.org/10.38124/ijsrmt.v5i6.1546*

# A Multi-Band 65 nm CMOS Power Amplifier Using Frequency Transformation Technique

Smail Traiche[1]

[1]Ecole Nationale Polytechnique, Center for Development of Advanced Technologies (CDTA), Algiers, Algeria.

Publication Date: 2026/07/25

**Abstract**

In this paper, a design and an optimization of feedback multi-band 65-nm CMOS power amplifier (PA) have been developed, based on the frequency transformation technique (FTT), in way to improve PA's performances. The FT Technique aims to transform an off-chip single-band matching networks considered as low-pass (LP) filters to that of triple-band matching networks (MN). An RC-feedback was firstly added in thourough manner to boost the linearity. An ideal simulations have led to good results in terms of different performances. In fact, after optimizations in the triple band MN and RC-feedback, PA's performances at central frequencies bands of 0.94, 1.94 and 2.44 GHz reached: (24.6 dBm, 24 dB, and 57.5%), (22.74 dBm, 20.48 dB and 48.9 %) and (25.8 dBm, 21.53 dB and 63.7 %), respectively. In addition, for the same central-frequencies, the output referred intermodulation third order point has given: 32.34, 22.06 and 32.34 dBm, respectively.

***Keywords:*** *65-nm CMOS, Multi-Band RC-FeedBack, Efficiency, Linearity, Frequency Transformation Technique, Third Order Intermodulation Point IMD3.*

## I. INTRODUCTION

During the recent two decades, mobile communication systems that integrate a multi-standards topologies have known a rapid development and wide spread either for low power systems as smart-phones, tablets and laptops, and for high power equipment systems [1] [2]. Indeed, low power mobile systems have especially seen a growth evolution in terms of multi-band and multi-power-mode circuits design techniques, taking into account standards specifications. Over time, second generation's (2G) protocols, as global system communication (GSM), are always existing in subsequent third/fourth (3G/4G) generations employing communication protocols, respectively [2]. Therefore, modern wireless communication systems require encompassing all protocols granted to the successive communication generations to one multi-band system in which, data (text, image, voice and video) should be transmitted.

Obviously, power amplifier as crucial part of transmitter, must be re-adapted to meet multi-band wireless communication systems specifications. In this context, several works are of interest in literature, to present PA topologies and techniques considering multi-standards concept. A dual-mode multi-band PA, using Envelop-Tracking (ET) technique, was designed for hand-set applications. ET technique has employed switching-capacitor technique to enhance linearity [3]. In [4] a frequency-agile RF front-end for time division duplexing (TDD), designed in the fully integrated 45nm SOI CMOS technology, is reported. A tunable switching macro/micro models active cores and an LC matching networks are proposed in [5] to cover 25 LTE bands and GSM. A class-E PA is implemented on the overall transmitter, dedicated to outdoor positioning applications, in which dual-band concept is ensured by frequency synthesizer PLL delivering 868 MHz and 2.4 GHz tones [6]. A tunable differential PA of which a resonant circuit formed of an inductor combined by switching capacitors, and tunable resistive feedback, are set up in [7], to constitute multi-band transmitter. The resistive feedback is also employed to adjust an input/output impedances to be fixed at 50 Ω. Hence, other works are mainly interested of using transformers as matching networks in way to attain high performance's PAs. The inter-digitated switchable transformer provides an optimum transformation impedance in four-band 2G/3G/4G/5G transmitter [8]. A multi-tap transformer is also employed in [9] to set up a class-E PA able to support triple-band concept. In [10] a triple-band CMOS differential-cascode PA is presented, adopting an Input-Output transformers combined with shunt-series lumped components to ensure an optimized wide-band input MN, and minimal passive output MN to obtain an optimized performed PA responding to CW, WCDMA, and LTE specifications. A Triple-band PA implemented with combiner, multi-tap, compact coupled L-shape concentric vertical (CL-CVT) and distributed active (DAT) transformers are presented in [11] - [13]. In fact, digitally-switchable capacitors, power cell resizing and aliasing-free digital pulse-width modulation techniques are employed thoroughly to demonstrate higher PA performances especially for the efficiency and linearity. The work reported in [14] ameliorated a linearity, by implementing two parallel switched blocks triple-band LDMOS PA. The average efficiency and the linearity are thus improved in the covered bands.

Purely lumped matching networks PAs are also proposed in [15] – [17], for the same concept. The first paper showed two stages LC-feedback power amplifier between which, reconfigurable lumped MNs are implemented to select GSM, GPS and WLAN operating bands. In the second paper, two stages (common-emitter, push-pull) PA, are thereby proposed, surrounded by reconfigurable MN ensuring 2 x 2 multiple input and multiple output for multi-band RF transceiver design used in the compact small cell base station. Moreover, multiband multimode (MMMB) PA in third paper, for GSM/TD-SCDMA/LTE cellular applications, using the π section interstage matching circuits and an on-chip passive lossy elements, by adding of parallel LC resonant circuits for the harmonic's suppression.

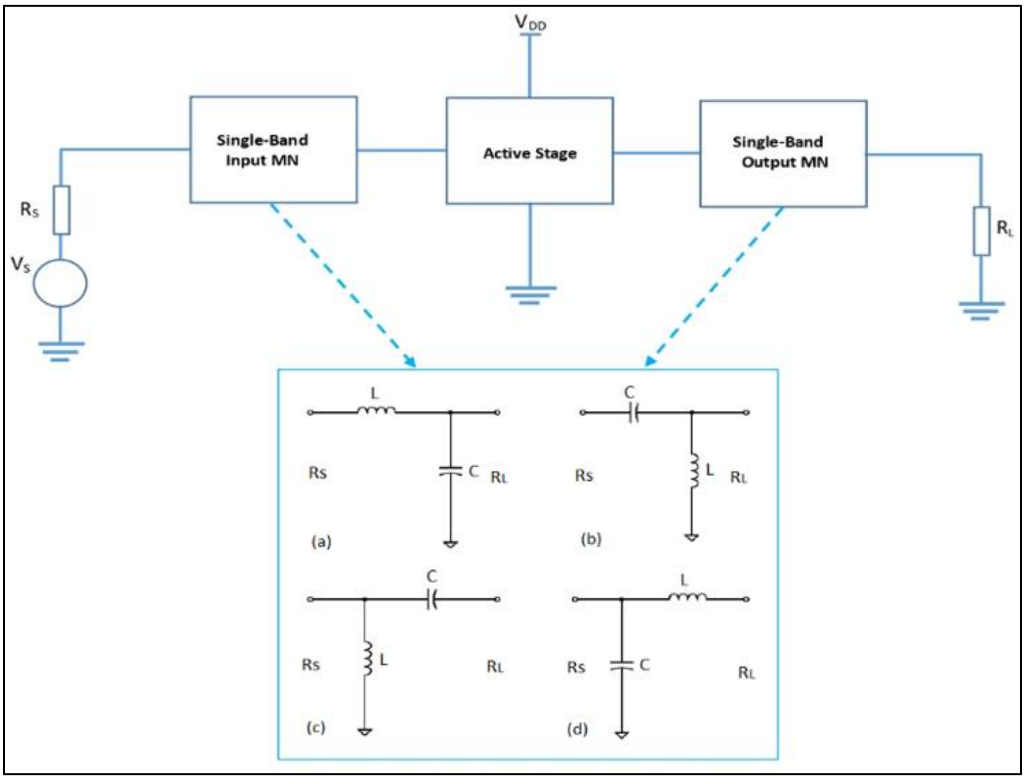


Fig 1 Form of Power Amplifier, with Possible Single-Band Matching Networks.

This paper presents a design and an optimization of triple-band 65 nm power amplifier using a frequency transformation technique, for GSM/WCDMA/LTE standards. Moreover, in section II, the proposed class-AB power amplifier with lowpass MNs performed by the frequency transformation technique. Section III will show simulation results and discussions. Finally, a conclusion of this work will be finally outlined in section VI.

## II. PROPOSED MULTI-BAND PA STRUCTURE

➢ *Single-Band Low-Pass L-MN Class-AB Power Amplifier*

In order to realize the triple-band power amplifier through frequency transformation concept, we must as first step, start to design narrow-band single frequency power amplifier. Indeed, L-Match network is a simple device responsible of maximal power's transformation from source to the load, for a given frequency [18] – [20]. Therefore, the possibilities of single-band lowpass and highpass filters, that serve as L-match networks arround an active stage, are depicted in Fig. 1. The selection of the possible structures is indicated regarding to the real part values of the input-output impedances of MN, $R_S$ and $R_L$ as follows If $R_S < R_L$: the structures mentioned in Fig. 1 (a) LPF-MN and (b) HPF-MN are suitable for the matching.

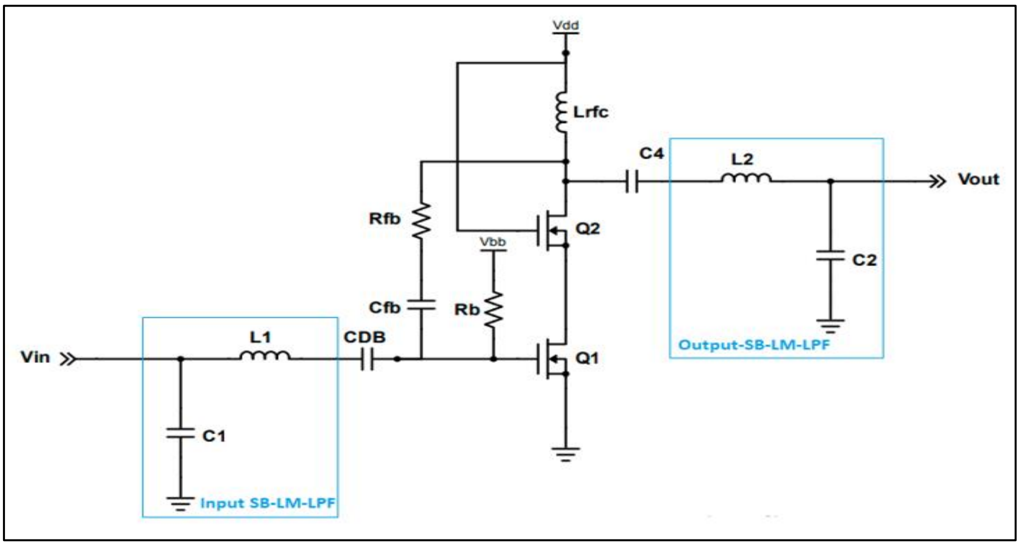


Fig 2 Single Band Power Amplifier, with Single-Band L-Match Low-Pass Filter Input and Output Networks.

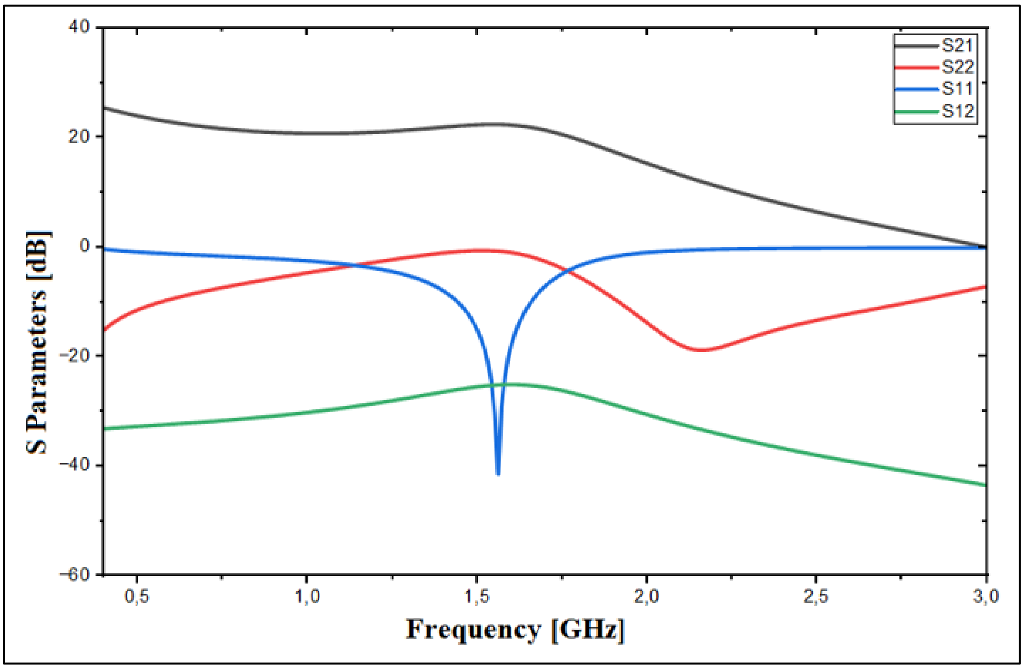


Fig 3 S-Parameters of Single-Band PA, for Frequency $f_m$ = 1.54 GHz.

If $R_S > R_L$: the structures mentioned in Fig. 1 (c) HPF-MN and (d) LPF-MN are suitable for the matching.

Where LPF-MN, HPF-MN mean Low-Pass Filter MN and High-Pass MN, respectively. To design this Single-Band PA, we have chosen a cascode topology of two transistors nmos-rf-25, which are of length L equal to 280 nm, and total width W of 320*12 µm as mentioned in Fig. 2. These important transistor dimensions and cascode topology are justified by high level of the output power for different targeted standards. By adopting the structures (a) and (d), which correspond to an LPF L-Match network, and represent the first step done for this work leading to design a single-band 65 nm CMOS PA. Hence, the S-Parameters for this PA are presented in Fig. 3, for matching frequency $f_m$ defined later as key parameter in the design of Triple-Band MN using frequency transformation technique. The RC-feedback is composed of a resistance $R_{fb}$ and capacity $C_{fb}$ optimized at 200 Ω and 400 fF, respectively. Networks L-Match ($C_1$, $L_1$) and ($C_2$, $L_2$) are implemented in the input and output of an active stage respecting the desired objective of triple-Band MN realization.

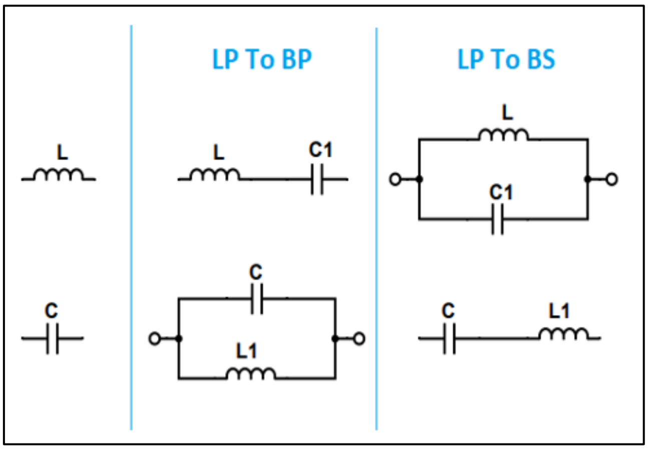


Fig 4 Possible Transformation Resonator Circuits, from Lowpass (LP) to Bandpass (BP) & Bandstop (BS).

➢ *Frequency Transformation Technique, Theory*

- *Dual-Band Transformation, Particular Case*

The frequency transformation technique is one to many frequency's variables [21]. Particularly, lowpass to bandpass and lowpass to stopband transformations are 1 → 2 mapping frequency variable. By studying this particular case as follows

For lowpass to dual-band bandpass transformation. This is given by the expression

$$\omega = \frac{\omega_t^2 - \omega_0^2}{\omega_t} \quad (1)$$

Where $\omega_t$ is mapped pulsation and $\omega_0$ is a center pulsation. This expression permits to transform an inductor to a series resonator circuit constituted of inductor-capacitor (with same inductor), and transform capacitor to parallel resonator circuit composed of inductor and capacitor arm (with same capacitor). Central pulsation of the resonator circuit is given by

$$\omega_0^2 = \frac{1}{LC_1} = \frac{1}{CL_1} \quad (2)$$

$C_1$ and $L_1$ are the new components of the transformed resonator circuits, as mentioned in Fig. 4. Expression (1) leads to a second order equation that can give two solutions, as mentioned below

$$\omega_t^2 - \omega_m\omega_t - \omega_0^2 = 0 \quad (3)$$

Where

$$\omega_m^2 = \frac{1}{LC\left(1 - \frac{1}{Q_0^2}\right)} \quad (4)$$

$\omega_m$ is the matching pulsation of L-Match LP Filter, in case of $R_S < R_L$ (Fig.1 (a)) as an example, and $Q_0$ is the loaded quality factor. Thus, the signs of the two solutions seem to be opposed, and the magnitude of positive solution is greater comparing to that of negative solution. Accordingly, these solutions are given by

$$\omega_1 - \omega_2 = \omega_m$$

$$\omega_1\omega_2 = \omega_0^2$$

These two solutions constitute a result of transformation from single-band L-Match LP Filter to Dual-Band BP Filter employed in the design of dual-band amplifiers.

For lowpass to dual-band bandstop transformation. This is given with the following formula.

$$\omega = \frac{\omega_0^2\omega_t}{\omega_0^2 - \omega_t^2} \quad (5)$$

As depicted in Fig. 4, an inductor of single-band LP is transformed to a parallel inductor and capacitor (keeping the same value of an inductance), and capacitor of single-band LP is transformed to series capacitor and inductor (with same kept capacitor's value) to compose dual-band bandstop BS filter MN. As previously, two solutions could occur for this second order equation.

$$\omega_t^2 + \frac{\omega_0^2}{\omega_m}\omega_t - \omega_0^2 = 0 \quad (6)$$

Which are

$$\omega_2 - \omega_1 = \frac{\omega_0^2}{\omega_m}$$

$$\omega_1\omega_2 = \omega_0^2$$

What present a dual-band bandstop filter employed as an eliminating circuit of two undesired frequencies.

- *Multi-Band MN Transformation, General Case*

Indeed, the impedance driving point remains the same for single-band or multi-band matching networks, by looking from both, source or load sides [21]. In addition, the frequency transformation technique for various load conditions, depends on the load impedance types regarding the sense of constant resistance or constant conductance circles in smith chart.

Substantially, there are three load impedance types

For parallel resistor-capacitor or series resistor-inductor loads:

This depends on the trace of an impedance load following impedance's traces (series resistor-inductor), or the admittance circle (parallel resistor-capacitor), (see Fig.5 (a)). We can deduce the generalized 1 → n mapping frequency transformation, which is given by

$$\omega = \frac{\omega_t^n + a_2\omega_t^{n-2} + a_4\omega_t^{n-4} + \cdots}{\omega_t^{n-1} + a_3\omega_t^{n-3} + a_5\omega_t^{n-5} + \cdots} \quad (7)$$

Where $\omega_t$ is a mapped transformed pulsation, and $n$ represents the number of bands, and $a_i$, such as: $i = 2$ *to* $n$ represent the transformation parameters. Thus, $\omega = \omega_m$ is the single-band matching pulsation before the transformation operation, and $\omega_i$ in the descending order are the mapped transformed pulsations corresponding to the obtained bands after the transformation.

The expression (7) leads to the polynomial expression

$$\omega_t^n - \omega_m\omega_t^{n-1} + a_2\omega_t^{n-2} - a_3\omega_m\omega_t^{n-3} + \cdots = 0 \quad (8)$$

Then, once matching pulsation $\omega_m$ and transformation parameters $a_i$ are calculated, we can build the mapping transformation to multi-band matching network as follow

$$\omega = \omega_t + \cfrac{1}{\cfrac{\omega_t}{a_{2-} a_3} + \cfrac{1}{\dots}} \quad (9)$$

In the case of seeking to find the transformed inductance or capacitance values L and C values, we multiply the two sides of expression (12) of jL or jC, respectively. This operation will illustrated well below when calculating the triple-band MN components.

For series resistor-capacitor or parallel resistor-inductor load. In general, the frequency transformation technique is suitable in the series, and parallel load according to Fig.5 (b). Therefore, the corresponding formula is given as

$$\omega = \frac{\omega_t + a_3\omega_t^3 + a_5\omega_t^5 + \cdots}{1 + a_2\omega_t^2 + a_4\omega_t^4 + \cdots} \quad (10)$$

To calculate the matching pulsation $\omega_m$ and the transformation parameters $a_i$, it would apply the same synthesis procedure with the previous section parallel RC or series RL load.

✓ *For Load Impedance Purely Resistive:*

Both kinds of mapping frequency transformation transformation shown above, are suitable for purely resistive load impedance in way to calculate different parameters.

➢ *An RC-Feedback Triple-Band PA Design Using Frequency Transformation Technique*

After taking in review the theoretical aspect of frequency transformation technique, we have to employ it in the designing of 65 nm CMOS PA, mentioned above, by producing the input-output matching networks accordingly. Therefore, the expected goal from this presented work is to design a PA that cover three bands of central frequencies corresponding to GSM, WCDMA and LTE, respectively. The adopted methodology is to perform the transformation of both input and output single-band MN built around matching frequency of $f_m$ = 1.54 GHz to input and output triple-band MN ($n$ = 3), as demonstrated in Fig. 5. For L-Match input matching network, the load impedance is a parallel RC defined as ($R_{11} \parallel (1/(jC_{gs1}\omega))$), where $R_{11}$ is a real part of input impedance ($Z_{11}$ = 10.71 – j8.17) of the input transistor $Q_1$, and $C_{gs1}$ is its gate-source capacitor.

Equivalent Triple-Band Network of ($L_1$, $C_1$) by applying expressions (7) - (10)

$$jL_1\omega = jL_1.\left[\omega_t + \cfrac{1}{\cfrac{\omega_t}{a_{2-} a_3} + \cfrac{a_3}{(a_{2-} a_3)\omega_t}}\right] \quad (11)$$

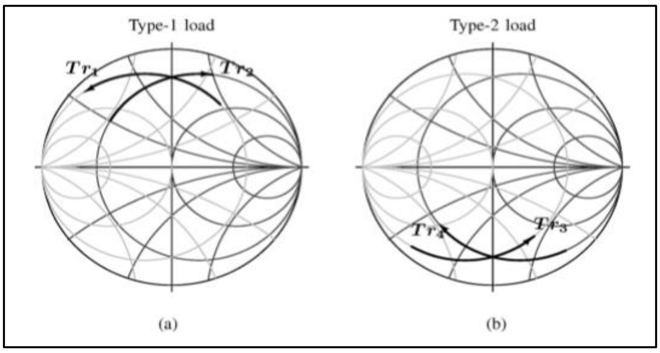


Fig 5 Impedances and Admittances Traces, (a) $Tr_1$ (Parallel Resistor-Capacitor), $Tr_2$ (Series Resistor-Inductor), (b) $Tr_3$ (Series Resistor Capacitor), $Tr_4$ (Parallel Resistor-Inductor) [21].

$$jC_1\omega = jC_1.\left[\omega_t + \cfrac{1}{\cfrac{\omega_t}{a_{2-} a_3} + \cfrac{a_3}{(a_{2-} a_3)\omega_t}}\right] \quad (12)$$

Furthermore

$$a_2 = -\omega_1\omega_2 - \omega_2\omega_3 + \omega_1\omega_3$$
$$a_3 = -\frac{\omega_1\omega_2\omega_3}{\omega_m}$$

And

$$\omega_m = \omega_1 - \omega_2 + \omega_3$$

After calculating $\omega_m$, $\omega_i$ and $a_i$ parameters (see Table. 1), the expressions (14) and (15) become

$$jL_1\omega = \left[j2.93.10^{-9}\omega_t + \cfrac{1}{j7.29.10^{-12}\omega_t + \cfrac{1}{j1.26.10^{-9}\omega_t}}\right]$$

$$jC_1\omega = \left[j6.05.10^{-12}\omega_t + \cfrac{1}{j3.51.10^{-9}\omega_t + \cfrac{1}{j2.62.10^{-12}\omega_t}}\right]$$

The same operation for the network ($L_2$, $C_2$) transformed to an output triple-band LPF matching network

$$jL_2\omega = \left[j2.58.10^{-9}\omega_t + \cfrac{1}{j8.25.10^{-12}\omega_t + \cfrac{1}{j1.11.10^{-9}\omega_t}}\right]$$

$$jC_2\omega = \left[j2.07.10^{-12}\omega_t + \cfrac{1}{j10.81.10^{-9}\omega_t + \cfrac{1}{j0.89.10^{-12}\omega_t}}\right]$$

This opration of frequency transformation has led the circuit shown in Fig. 2 to that illustrated in Fig. 6. Moreover, the triple-band matching networks are implemented following the off-chip form, considering the number of inductors in the PA circuit in addition of the RFC inductor. However, the implementation in the on-chip form, of inductors will degrade consequentelly the PA's performances. As mentioned above, the input single-band matching network ($L_1$, $C_1$) is transformed to its corresponding network composed of; parallel ($L_{1P1}$, $C_{1P1}$ and $C_{1P2}$), series ($L_{1S1}$, $L_{1S2}$ and $C_{1S1}$). Whereas the output matching network ($L_2$, $C_2$) to that of series ($L_{2S1}$, $L_{2S2}$ and $C_{2S1}$) and parallel ($L_{2P1}$, $C_{2P1}$ and $C_{2P2}$), while the feedback components are fixed at 200 Ω and 400 fF for $R_{fb}$ and $C_{fb}$, respectively. Table I summerizes the parameters and Triple-Band MN components values that caracterize the designed power amplifier matching can be remarked for the three frequencies of interest whether for the input Triple-Band MN in Fig. 7 (a), and the output transformation, from the purely resistive load (resistive load-line in I-V characteristics of transistor $Q_1$) to 50 Ω in way to extract a maximum output power from the active stage instead of a maximum efficiency. Therefore, $S_{22}$ can not be consisdered as well matched parameter for the three frequencies in this case.

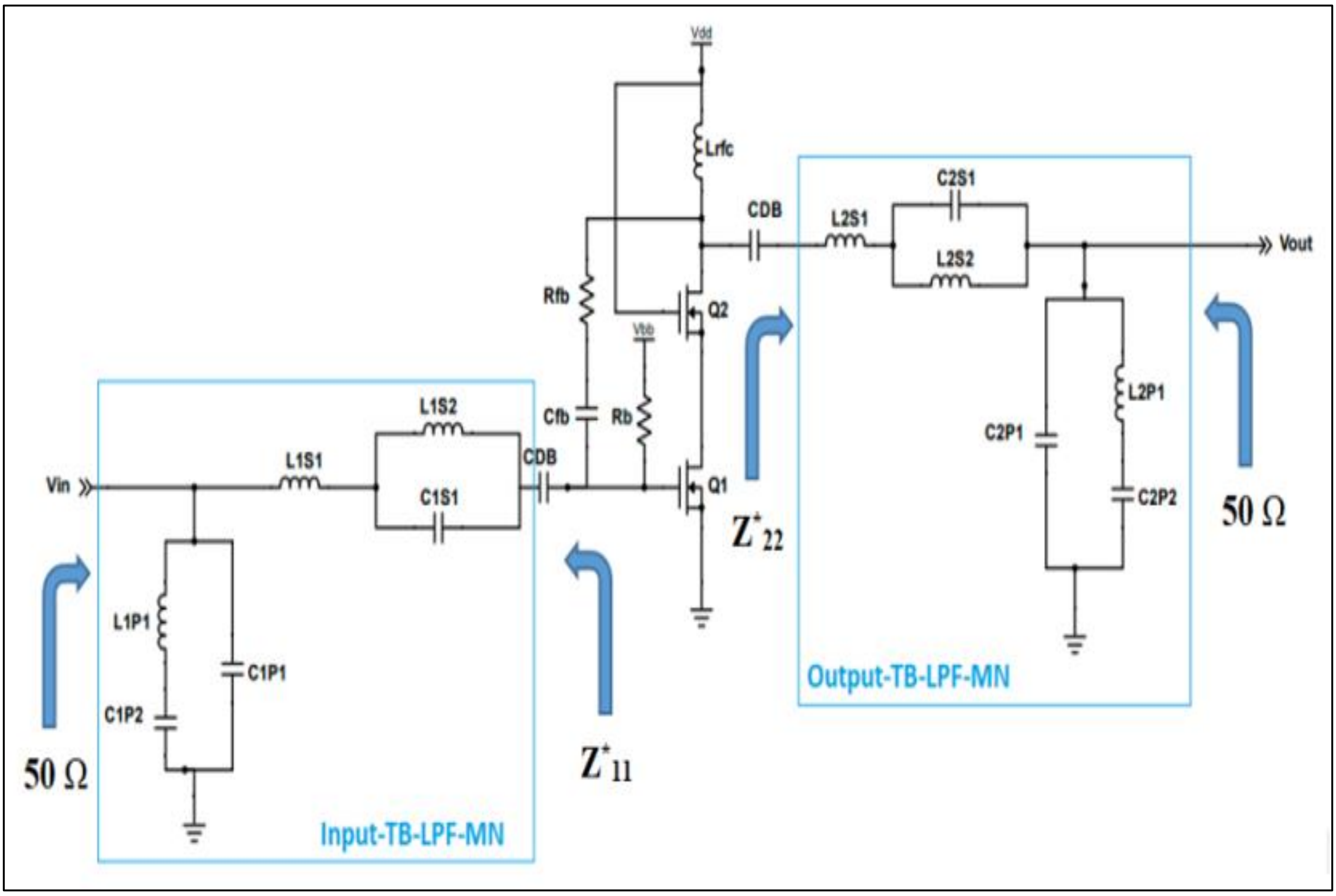


Fig 6 The Overall Triple-Band PA After Applying a Frequency Transformation Technique.

## III. TRIPLE-BAND RC-FEEDBACK PA, SIMULATIONS AND RESULTS

➢ *Simulations and Results Before Optimization*

After dimensionning the triple-band PA input-ouput matching networks, their S-Z ideal parameters were simulated using cadence virtuoso. The results are illustrated in Fig. 7. In fact, the input matching network S-Z parameters are extracted between 50 Ω (as characteristic impedance) and $Z_{in} = Z^*_{11} = 10.71 + j8.17$ Ω, composed of ($R_{11} \| (1/jC_{gs1}\omega)$), considering it as an input impedance of a cascode topology, while the output mathing network's ones are taken between $Z_{out} = Z^*_{22} = 24.71 + j12.91$ Ω and 50 Ω. Hence, a better matching can be remarked for the three frequencies of interest whether for the input Triple-Band MN in Fig. 7 (a), and the output transformation, from the purely resistive load (resistive load-line in I-V characteristics of transistor $Q_1$) to 50 Ω in way to extract a maximum output power from the active stage instead of a maximum efficiency. Therefore, $S_{22}$ can not be consisdered as well matched parameter for the theree frequencies in this case. The overall triple-band PA S-Parameters are depicted in three concerned frequencies. In fact, the most better performances are obtained for an opperating frequency of 0.94 Fig. 8. From that, the good matching is clearly remarked especially for the frequency 2.44 GHz regarding to $S_{11}$ parameter, which seems lower than – 10 dB, and $S_{21}$ parameter attaining 18.32 dB that is considered as better gain. However, an acceptable matching is obtained for the two frequencies 0.94 for which insertion losses are slightely greater than – 10 dB and $S_{21}$ is around 17 and 23 dB, respectively. triple-tand PA performances are thus illustrated in Fig. 9. These are mainly represented by an output power (blue lines), power gain (red lines) and an efficiency with (black lines) for GHz (dotted lines), where maximal efficiency exceeds 57 % at the maximal power (load) level, which equal to 23 dBm, corresponding of power gain level of 16 dB.

Table 1 Triple-Band RC-Feedback PA Parameters and Components Values.

| **Parameter** | $\omega_1$ (rad/s) | $\omega_2$ (rad/s) | $\omega_3$ (rad/s) | $\omega_m$ (rad/s) | $f_1$ (Hz) | $f_2$ (Hz) | $f_3$ (Hz) | $f_m$ (Hz) | $a_2$ (rad/s)$^2$ |
|---|---|---|---|---|---|---|---|---|---|
| **Value** | $1.53\ .10^{10}$ | $1.22.10^{10}$ | $0.52.10^{10}$ | $0.96.10^{10}$ | $2.44.10^{9}$ | $1.94.10^{9}$ | $0.84.10^{9}$ | $1.54.10^{9}$ | $-1.08\ 10^{20}$ |
| **Parameter** | $a_3$ (rad/s)$^2$ | $L_1$ (H) | $C_1$ (F) | $L_2$ (H) | $C_2$ (F) | $L_{1P1}$ (H) | $C_{1P1}$ (F) | $C_{1P2}$ (F) | $L_{1S1}$ (H) |
| **Value** | $-1.54\ 10^{20}$ | $2.93.10^{-9}$ | $6.08.10^{-12}$ | $2.58.10^{-9}$ | $2.07.10^{-12}$ | $3.51.\ 10^{-9}$ | $6.05.10^{-12}$ | $2.62.10^{-12}$ | $6.05.\ 10^{-9}$ |
| **Parameter** | $L_{1S2}$ (H) | $C_{1S1}$ (F) | $L_{2S1}$ (H) | $L_{2S2}$ (H) | $C_{2S1}$ (F) | $L_{2P1}$ (H) | $C_{2P1}$ (F) | $C_{2P2}$ (F) | $L_{rfc}$ (H) |
| **Value** | $1.26.\ 10^{-9}$ | $7.29.10^{-12}$ | $2.58.10^{-9}$ | $1.11.\ 10^{-9}$ | $8.25.10^{-12}$ | $10.81.\ 10^{-9}$ | $2.07.10^{-12}$ | $0.89.10^{-12}$ | $15.\ 10^{-9}$ |

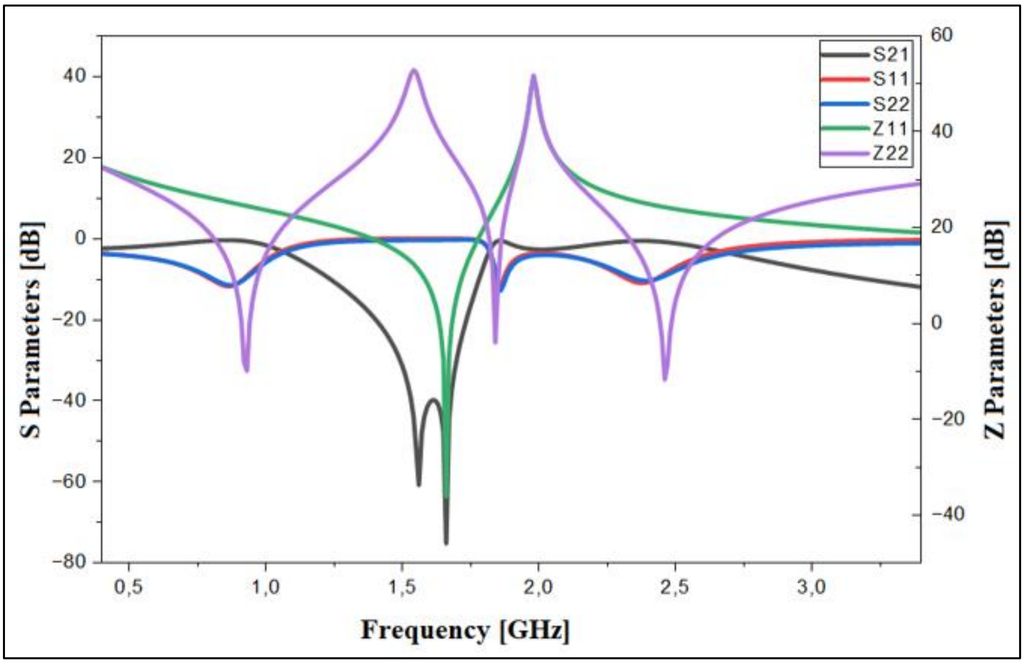


(A)

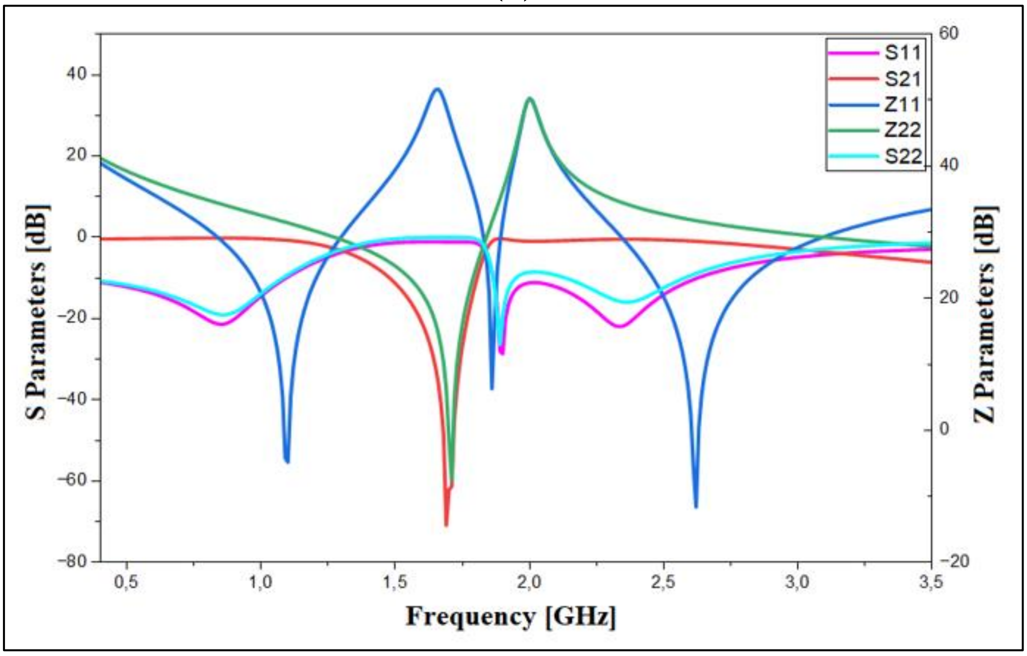


(B)

Fig 7 S and Z Parameters for Triple-Band Matching Networks After Applying a FTT; a) Input MN, b) Output MN.

Meanwhile, these performances reduce as well for the frequencies 1.94 (solid lines) and 2.44 GHz (dashed lines)

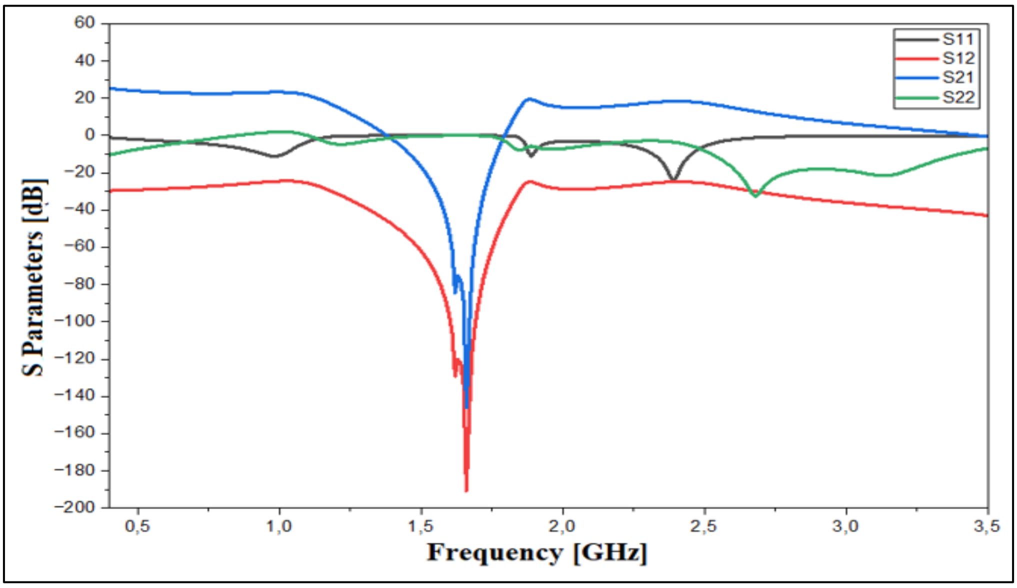


Fig 8 S Parameters for Triple-Band PA After Applying FTT.

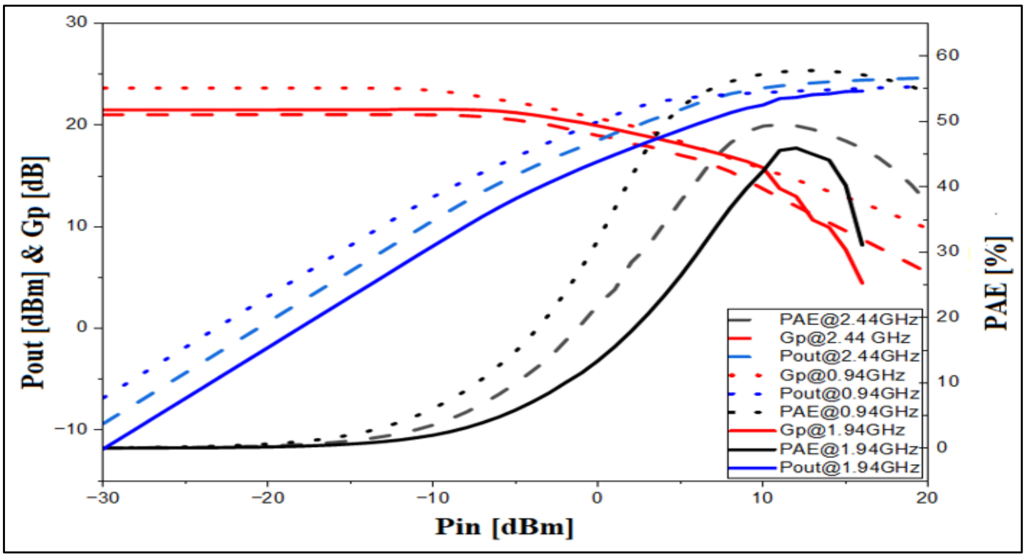


Fig 9 Triple-Band PA Performances After Applying FTT for the Three Frequencies 094, 1.94 and 2.44 GHz.

Comparing to the first one, and that because the fact of, as the frequency increases, the delivered energy and therefore power.

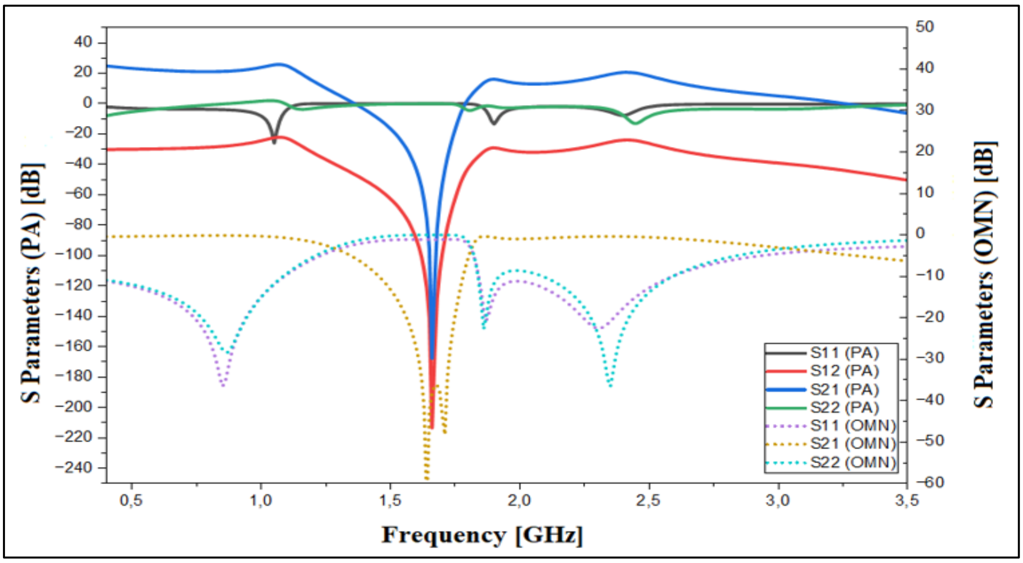


Fig 10 S Parameters for Triple-Band PA (Solid Lines), Output Matching Network OMN (Dotted Lines), After Optimizations.

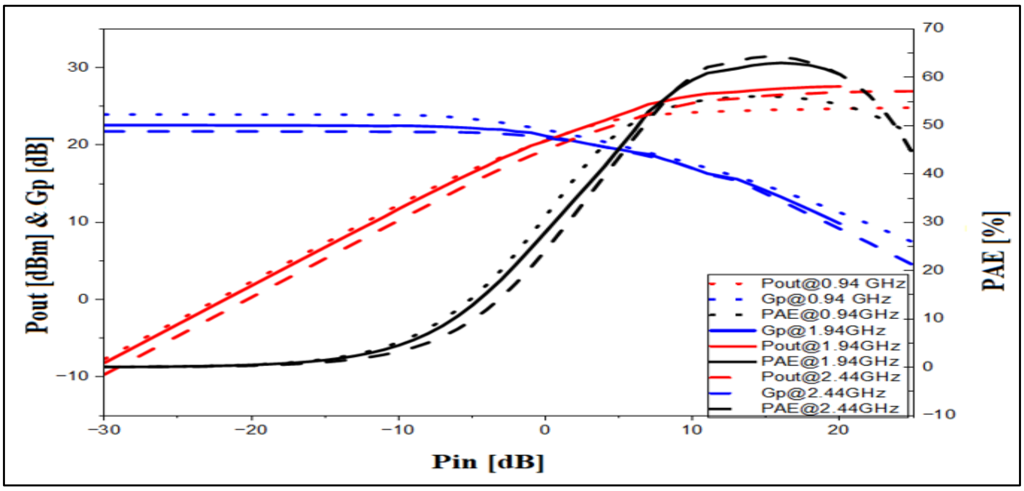


Fig 11 Triple-Band PA Performances for the three Frequencies 094, 1.94 and 2.44 GHz, After Optimization.

Decrease, following an inverse relationship. Accordingly, the maximal efficieny reaches 49.52 % corresponding to the maximal power of 23.85 dBm, and the power gain of 12.87 dB (frequency equal 2.44 GHz). In addition, the maximal effecienty of around 46 % is attained for a saturated Pout of 23 dBm, corresponding to power gain of almost 13 dB By regarding the linearity as peformance, it is observed a slight poor linearity for this preliminary's case. Moreover, this drawback is marked by a gap between a compressed point and saturated-point of both; an output power and power gain in three band-center frequencies.

➢ *Triple-Band PA Design, the Optimization*

The optimization of the proposed is performed using an output matching network devices, tunable capacitors implemented upon small chip areas and inductors of an output series branch.

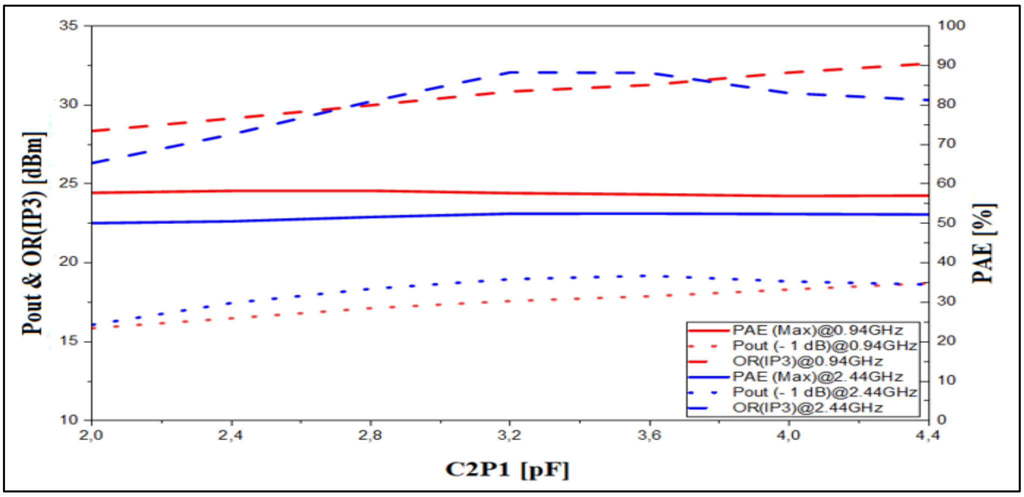


(A)

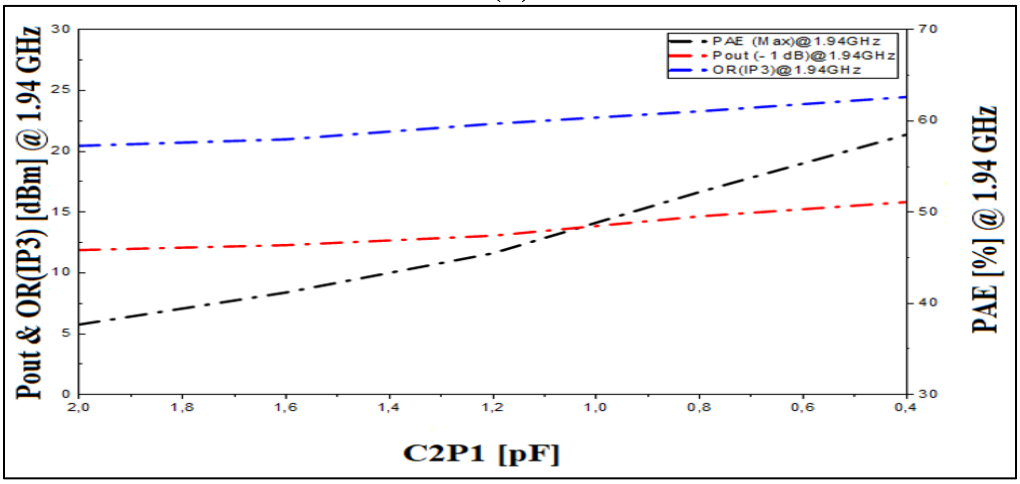


(B)

Fig 12 Triple-Band PA Performances; PAE, Pout (-1dB) and OR (IP3), a) for the Frequencies 094, 2.44 and b) 1.94 GHz, After Optimization by Capacitance $C_{2P1}$.

Therefore, capacitors $C_{2S1}$, $C_{2P1}$ and inductors $L_{2S1}$ and $L_{2S2}$ (see Fig. 6) have been selected in order to improve PA performences. In fact, adjusting these devices values will reduce the par ameters $S_{11}$ and $S_{22}$ of an output matching network marked by dotted lines in Fig. 10. These two parameters are reduced under -20 dB for 0.94, 1.94 and 2.44 GHz.

Consequently, an overall PA's maximal power added efficiency was enhanced to exceed 60 % for frequencies 1.94 and 2.44 GHz (see black dashed and solid lines in Fig. 10), and 50 % (black dotted line in same figure) for frequency 0.94 GHz. At same time, an output power is also enhanced to exceed 25 dBm for three frequencies (red lines in Fig. 11), what respond carfully to the standard specifications. The remarqued improvements in triple-band PA performances are refered to the efficacy of the optimization at the output matching network (OMN), for which one could seek the reason. In other words, why the OMN is selected for an optimization?, because of signal's power at the output is more powerful thanks to an active stage and voltage supply, where its shaping through OMN's devices become more efficiente than an input MN ones.

Table 2 Compoaison of Proposed Triple-Band RC-Feedback Pa Results with the State-of-the-Art Results.

| Ref. | Technology | Frequency (GHz) | $V_{DD}$ (V) | $P_{DC}$ (mW) | $P_{out}$ (sat)/ $P_{out}$(-1dB) (dBm) | OR(IIP3) (dBm)/ ACLR (dBc)/EVM (%) | PAE (%) | Area ($mm^2$) | class | Technique |
|---|---|---|---|---|---|---|---|---|---|---|
| [7] | 0.18 µm CMOS | 0.9 – 3<br>4 Bands | 3.3 | - | 20 - 21 | - | 11 - 23 | 0.31 | - | Feedback, Tunable Output Matching Network |
| [9] | 0.18 µm CMOS | 0.8<br>1.9<br>2.4 | 3.3 | - | 28<br>29.6<br>26.5 | - | 40<br>45<br>37 | 2.25 | E | Output Multi-Tap Transfomer Combiner |
| [10] | 0.18 µm CMOS | 0.95<br>1.8<br>2.4 | 3.2/3.3 | - | -/25.3 – 27.2<br>-/23.5 – 26.6<br>-/20 | -/-33 -30/-<br>-/ -33 -30/-<br>-/-/3.98 | 14 – 29<br>23.6 – 30.6<br>20 | 1.68 | - | Output switchable matching network |
| [11] | 0.065 µm CMOS | 2.5<br>3<br>3.5 | 1.2 | - | 22.5/-<br>21.5/-<br>21.5/- | - | 16.5<br>15<br>15 | 2.88 | AB/C | Reconfigured output combiner transformer |
| [12] | - | 1.8<br>1.9<br>2.6 | 3.3 | - | 27.8/-<br>28.1/-<br>27.4./- | -/-34 -48/-<br>-/-35.8 -51/-<br>-/-34 -48/- | 31<br>34.5<br>29.2 | 2.772 | E | Output Matching Network based on Differential tuned combiner Transfomer |
| [22] | - | 0.98<br>1.4<br>1.9 | 1.8 - 3.6 | - | 26 /24.5<br>26/24.5<br>26//24 | - | 20<br>20<br>18 | 5.1 | - | Switching two Input-Output Matching Network |
| This Work | - | 0.94<br>1.94<br>2.44 | 2.5 | 716 | 24.7/18.71<br>27.3/17.24<br>26.4/18.63 | 32.63/-/-<br>24.48/-/-<br>32.07/-/- | 56.13<br>63<br>64.3 | - | AB | Input-Output Matching Networks Based on Frequency Transformation Technique |

➢ *Triple-Band PA, Linearity Improvement*

Another parameters are introduced to assess and ameliorate the triple-band PA linearity for the three frquencies are; the third order intermodulation point beside the output power compression one. In this way, a capacitor $C_{2P1}$ in the ouput matching network was only choosed to optimize the linearity, as depicted in Fig. 12(a). and the same capacitor was inversely varied from 2 → 0.2 pF to improve linearity for frequency 1.94 GHz in the other hand. Consequentely, for frequency 0.94 GHz, the output compression point and the output refered IP3, increase with $C_{2P1}$ evolution, from 15.71 dBm to practically 19 dBm and 28.36 dBm to 32.63 dBm, respectively. However, for the frequency 2.44GHz, these two parameters reach theirmaximum values, that are 19.09 and 32.07 dBm, respectively, corresponding to $C_{2P1}$(3.2, 3.6 pF), and drop slightly for the rest. Moreover, Fig.12 (b) illustrates an evolution of the above mentioned parameters using capacitor $C_{2P1}$ for frequency 1.94 GHz. In fact, $P_{out}$(-1dB) and OR(IP3) increase inversely with $C_{2P1}$ from 11.9 to 15.84 dBm and 20.47 to 24.48 dBm, respectively. This responds to the LTE specifications considering a poor linearity knowing that saturated output power exceeds 24 dBm. For the whole, the important gap between $P_{out}$(-1dB) and OR(IP3) represents a good sign of linearity of this triple-band PA.

## IV. DISCUSSIONS

As for comparing this work with literature in Table 2, and taking into the account several parameters that describe the PA's operating, mentionning that overall articles are designed in CMOS process upon three bands (triple-bands) context. By starting with most important parameter, which is the output power, the presented work reveals an acceptable levels of power sat 24.7, 27.3 and 26.4 dBm for frequencies 0.94, 1.94 and 2.44 GHz, respectively. However, the output power compressed points remain insufficient, necessitating therefore a linearisation techniques to minimise a gap between compressed and saturated output power levels. Such results are near to that obtained in [9] and [10], which are evaluated between 29.6 and 26.5 dBm for the first one, and compressed point between 20 and 27.2 dBm for second one. Mentionning that its design is performed in 0.18 µm CMOS process. Hence, PAs shown in [12] and [22] are nearly for same level comparing to that mentionned above, regarding always 0.18µm & 0.35 µm CMOS technology, that allow reaching higher output power levels than 0.65 nm CMOS.

Power added efficiency is also a principle key parameter that examines Triple-Band PA performances, based on frequency transformation technique, which demonstrates better levels of the efficiency comparing to other works. Therefore, results give 56.13, 63 and 64.3 % for frequencies 0.94, 1.94 and 2.44 GHz, respectively. Such results are obtained by considering that the two input and output matching networks are mounted off-chip unlike works comparing-with, that are on the whole of on-chip inserted matching networks. In fact, respectible levels of an efficiency are observed in [9] and [12], that are of 40, 45 and 37 % for 0.8, 1.9 and 2.4 GHz, and 31, 34.5 and 29.2 % for, for WCDMA and LTE applications, respectively.

Although using transformers-combiners especialy in an output matching network occupy a large chip's surface, they preserve PA efficiency considering their high quality factor. In the rest of works, a weak efficiency is remareked. As for the work reported in [7], the fact of using differential pair, switching capacitors and an important number of resistors degrade consequentely the overall PA's efficiency. In [11], the PA is designed using 65 nm CMOS technology while employing several integrated transformers, that give-off a huge amounts of energy under magnetic and resistive losses leading to degrade an overall efficiency. Thus, in [22] an important number of integrated inductors in both, two switched input and output matching networks reduce the efficiency to arround 20 %. The linearity treated by three different parameters, is taken in the consideration to evaluate a triple-band PA's performances, (IP3), (ACLR) and de (EVM). Among those, IP3 is used to mentionne the designed PA, of which results presented refered order IP3 worth 32.53, 24.48 and 32.07 dBm for three bands 0.94, 1.94 and 2.44 GHz, respectively. An obtained results reveal a good linearity by view of large gap between $P_{out}$(-1dB) and OR(IIP3) points. However, an unsufficient $P_{out}$(-1dB) for the three frequencies that don't reach 20 dBm necessary to cover GSM, WCDMA and LTE standards specifications. Comparing to the works presented in Table 2, [10] illustrates a good ACLR that worth -33 to -30 dBc for two bands 0.94 and 1.8 GHz, and EVM within standards of 3.98 % for the band 2.4 GHz. In same context, [12] presents more better linearity than previous article linearity according to ACLR parameter. In fact, this metric worth (-34, -48) dBc for band 1.8 GHz, with offset frequency of (5, 10) MHz, respectively, and (-34, -48) dBc for band 2.4 GHz for same offset frequency corresponding the LTE standard. Also, for band 1.9 GHz corresponding to WCDMA, ACLR worth (-35.8, -51) dBc for an offset frequency of 5, 10 MHz, respectively.

## V. CONCLUSION

In this work, an RC-feedback triple-band 65 nm CMOS class-AB power amplifier has been designed by starting from an RC-feedback single-band power amplifier, and adopting a frequency transformation technique (FTT). Such technique allowed cearting two input-output matching networks under forms of low-pass filters to that of an off-chip triple-band under forms of bandpass filters, of center frequencies of 0.94, 1.94 and 2.44 GHz. These bands are dedicated to cover GSM, WCDMA, LTE and even ZigBee/BLE, ISM standards. Consequentely, the proposed PA reveals good performances in terms of a maximal power in the load, gain and efficiency are quoting of (24.7, 27.3 and 26.4) dBm, (11.26, 13.27 and 13.65) dB and 26.4) and (56.13, 63 and 64.3) % corresponding respectively to 0.94, 1.94 and 2.44 GHz bands. In addition, the linearity is carachtirized by a third order intermodulation point that is mentionned at (32.63, 24.84 and 32.04) dBm for same bands. However, linearity is slightly poor for band 1.94 GHz because it does not cover the overall intervall allocated to the LTE standard, what necessitate more enhancement in terms of linearity. As perspectives, this work demands more improvements, in hand, to add more possible bands (quad-band PAs for example) with examination of their performances, and try to implement matching networks combinations; lowpass/highpass, highpass/lowpass and highpass/highpass filters, for the future works.

## REFERENCES


[1]. G.Han, X.G.Yin and T.Lin, ″Study on Medium Voltage Power-line Based Communication System Scheme for Power Distribution Automation and Development ofits Terminal Equipment″, International Conference on Power System Technology, vol. 60, no. 6, pp. 1784–1796, 22-26 October 2006. DOI: 10.1109/ICPST.2006.321687, Chongqing, China.

[2]. L.Yohann, Contribution ″a la réalisation d'amplificateurs de puissance en technologie CMOS 65 nm pour une application au standard UMTS″, Thèse soutenue en 2009, ÉCOLE DOCTORALE DE SCIENCES PHYSIQUES ET DE L'INGENIEUR, Université de Bordeaux, France.

[3]. Y.Cho, D.Kang, J.Kim, D.Kim, B.Park and B.Kim, ″A Dual Power-Mode Multi-Band Power Amplifier With Envelope Tracking for Handset Applications, IEEE Transactions on Microwave Theory and Techniques″, Page(s): 1608 – 1619, DOI: 10.1109/TMTT.2013.2250712, 19 March 2013.

[4]. S.Goswami, H.im, J.L.Dawson. ″A frequency-agile RF frontend for multi-band TDD radios in 45nm SOI CMOS. 2013 IEEE Radio Frequency Integrated Circuits″, Symposium (RFIC), 02-04 June 2013, DOI: 10.1109/RFIC.2013.6569596, Seattle, WA, USA.

[5]. S.B.Hamidi, D.Dawn, ″Fully integrated LTE-band CMOS tunable power amplifier″, 2017 IEEE 18th Wireless and Microwave Technology Conference (WAMICON), 24-25 April 2017. DOI: 10.1109/WAMICON.2017.7930263, Cocoa Beach, FL, USA.

[6]. C.Y.Hsieh, J.Roeber, A.Baenisch, A.Hagelauer, T.Ussmueller, ″A low power CMOS transmitter with Class-E power amplifiers for positioning application in multi-band″, 2016 German Microwave Conference (GeMiC), 14-16 March 2016, DOI: 10.1109/GEMIC.2016.7461648, Bochum, Germany.

[7]. D.Imanishi, K.Okada, A.Matsuzawa, ″A 0.9–3.0 GHz fully integrated tunable CMOS power amplifier for multi-band transmitters″, 2009 IEEE Asian Solid-State Circuits Conference, 16-18 November 2009, DOI: 10.1109/ASSCC.2009.5357277, Taipei, Taiwan.

[8]. W.Jung, S.Kang, D.Jeong, K.Y.Son, J.Lee and J.Lee, ″A Sub-6GHz 5G New Radio Multi-Band Transmitter with a Switchable Transformer in 14nm FinFET CMOS″, 2021 IEEE Radio Frequency Integrated Circuits Symposium (RFIC), 07-09 June 2021, DOI: 10.1109/RFIC51843.2021.9490416, Atlanta, GA, USA.

[9]. W.Y Kim, H.S.Son, J.H.Kim, J.Y.Jang, I.Y.Oh, C.S.Park, ″A Fully Integrated Triple-Band CMOS Class-E Power Amplifier With a Power Cell Resizing Technique and a Multi-Tap Transformer″, IEEE Microwave and Wireless Components Letters ( Volume: 23, Issue: 12, December 2013), Page(s): 659 - 661, DOI: 10.1109/LMWC.2013.2283874.

[10]. M.Lee, C.Park, ″A Triple-Band CMOS Power Amplifier Using Multi-Band and Switchable Matching Network for Wireless Mobile″, IEEE Transactions on Microwave Theory and Techniques, ( Volume: 67, Issue: 10, October 2019), Page(s): 4220 - 4231, DOI: 10.1109/TMTT.2019.2931899.

[11]. R.Singh, J.Paramesh, ″A digitally-tuned triple-band transformer power combiner for CMOS power amplifiers″, 2017 IEEE Radio Frequency Integrated Circuits Symposium (RFIC), 04-06 June 2017, DOI: 10.1109/RFIC.2017.7969085, Honolulu, HI, USA.

[12]. H.S.Son, W.Y.Kim, J.Y.Jang, I.Y.Oh, C.S.Park, ″A triple-band CMOS class-E power amplifier for WCDMA/LTE applications″, 2013 Asia-Pacific Microwave Conference Proceedings (APMC), 05-08 November 2013,. DOI: 10.1109/APMC.2013.6694824, Seoul, Korea (South).

[13]. H.S.Yang, Y.J.E.Chen, J.H.Chen, A Pulse-Mode CMOS Power Amplifier for Multi-Band LTE Femtocell Base Stations, 2016 IEEE MTT-S International Microwave Symposium (IMS), 22-27 May 2016, DOI: 10.1109/MWSYM.2016.7540384, San Francisco, CA, USA.

[14]. K.Kim, D.H.Lee, S.Hong, ″A Dual-Mode Multi-Band Second Harmonic Controlled SOI LDMOS Power Amplifier″, IEEE Microwave and Wireless Components Letters ( Volume: 25, Issue: 7, July 2015), Page(s): 466 - 468. DOI: 10.1109/LMWC.2015.2429115.

[15]. Zhangfa Liu, Jing Wang, A reconfigurable multi-band CMOS power amplifier design, 2011 International Conference on Electric Information and Control Engineering, 15-17 April 2011, DOI: 10.1109/ICEICE.2011.5777325, Wuhan, CHINA.

[16]. K.Lim, H.D.Lee, H.Ahn, S.Lee, S.Jang, S.Baek, B.Moon, Y.Lee, H.Shin, S.Kim, J.Lee, H.Lee, K.Kang, H.Shim, C.Sung, G.Park, G.Lee, M.Kim, S.Park, H.Jung, O.Lee, B.Park, and J.Lee, ″A 2×2 MIMO multi-band RF transceiver and power amplifier for compact LTE small cell base station″, 2017 IEEE International Symposium on Radio-Frequency Integration Technology (RFIT), 30 August 2017 - 01 September 2017. DOI: 10.1109/RFIT.2017.8048282.

[17]. JLin, Y.Zheng, Z.Zhang, G.Zhang, ″A multi-mode multi-band power amplifier for quad-band GSM, dual-band TD-SCDMA, and TDD LTE band 39 cellular applications, 2015 Asia-Pacific Microwave Conference (APMC), 06-09 December 2015″, DOI: 10.1109/APMC.2015.7411817.

[18]. J.Xiao, M.Liu, Z.Zhu, ″A 9-22GHz Ultra-WideBand Power Amplifier with Diode Linearier for Multi-Band PLL Driver″, 2019 IEEE International Conference on Electron Devices and Solid-State Circuits (EDSSC), 12-14 June 2019, DOI: 10.1109/EDSSC.2019.8754430.

[19]. D.M.Pozar, ″Microwave Ingineering″, Fourth Edition, ISBN 978-0-470-63155-3 (hardback : acid free paper) Dec. 2011, John Wiley & Sons, Inc.
[20]. G.Gonzalez, ″Microwave Transistor Amlifiers Analysis and Design″, TK7871.2.G59 1984, ISBN: 0-13-581646-7, by printice-Hall, Inc, Englewood Cliffs, New Jeresy 07632, USA.
[21]. N.Nallam, S.Chatterjee, ″Multi-Band Frequency Transformations, Matching Networks and Amplifiers″, IEEE Transactions on Circuits and Systems I: Regular Papers ( Volume: 60, Issue: 6, June 2013), Page(s): 1635-1647, Feb. 2015, DOI: 10.1109/TCSI.2012.2221175.
[22]. S.B.Hamidi, D.Dawn, ″A Fully-Integrated Reconfigurable CMOS Power Amplifier Utilizing a Novel Impedance Matching Topology″, 2022 IEEE 15th Dallas Circuit And System Conference (DCAS), 17-19 June 2022, DOI: 10.1109/DCAS53974.2022.9845544, Dallas, TX, USA.